

Orbital ferromagnetism and anomalous Hall effect in antiferromagnets on distorted fcc lattice

Ryuichi Shindou¹ and Naoto Nagaosa^{1,2}

¹ Department of Applied Physics, University of Tokyo, Bunkyo-ku, Tokyo 113-8656, Japan

² Correlated Electron Research Center, Tsukuba, Ibaraki 303-0046, Japan

(May,1,2001)

The Berry phase due to the spin wavefunction gives rise to the orbital ferromagnetism and anomalous Hall effect in the non-coplanar antiferromagnetic ordered state on face-centered-cubic (fcc) lattice once the crystal is distorted perpendicular to (1,1,1) or (1,1,0)- plane. The relevance to the real systems γ -FeMn and NiS₂ is also discussed.

PACS numbers: 11.30.Er, 11.30.Rd, 75.30.-m, 71.27.+a

It has been recognized for a long term that the chirality plays important roles in the physics of frustrated spin systems [1–6]. These degrees of freedom are distinct from the (staggered) magnetization, and could show phase transition without magnetic ordering [1–3]. Especially since the discovery of the high-T_c cuprates, the scalar spin chirality

$$\chi_{ijk} = \vec{S}_i \cdot (\vec{S}_j \times \vec{S}_k) \quad (1)$$

has been a key theoretical concept in the physics of strongly correlated electronic systems [4–6]. This spin chirality acts as the gauge flux for the charge carriers moving in the background of the fluctuating spins. In order for the spin chirality χ_{ijk} to be ordered, both the time-reversal (T) and parity (P) symmetries must be broken. Broken T and P symmetries in 2D bring about many intriguing physics such as parity anomaly [7,8], anyon superconductivity [9], and quantized Hall effect *without* external magnetic field [10]. A physical realization of the last one has been discussed [11] in the context of anomalous Hall effect (AHE) in ferromagnets via the spin chirality mechanism [12–15].

In this paper we explore the chiral spin state in the ordered antiferromagnet (AF) on the three-dimensional face-centered-cubic (fcc) lattice. The AF on the fcc lattice is a typical frustrated system, and nontrivial spin structure with the finite spin chirality in eq.(1) is expected. For example, in the charge transfer (CT) insulator NiS₂ [16] and in the metallic alloy γ -FeMn [17] the non-coplanar spin structure (so-called triple-Q structure shown in Fig. 1a) has been observed. A theoretical explanation for this structure is the following. Let us consider the case where the lattice points are divided into 4-sublattices as shown in Fig. 1a. Denoting the (classical) spin moment at each sublattice as \vec{S}_a ($a = 1, 2, 3, 4$), the 2-spin exchange interaction energy is written as $H_2 \propto (\sum_{a=1,4} \vec{S}_a)^2$. Therefore the condition of the lowest energy $\sum_{a=1,4} \vec{S}_a = \vec{0}$ does not determine the spin structure and leaves many degenerate lowest energy configurations. Then the interactions which lift this degeneracy such as the 4-spin exchange

interaction become important [18,19]. In particular the phenomenological Ginzburg-Landau theory for the 4-spin exchange interaction is given as $H_4 = J_4 \sum_{a \neq b} (\vec{S}_a \cdot \vec{S}_b)^2$ [19]. With positive J_4 , the ground state configuration is given by $\vec{S}_1 = (\frac{1}{\sqrt{3}}, \frac{1}{\sqrt{3}}, \frac{1}{\sqrt{3}})$, $\vec{S}_2 = (\frac{1}{\sqrt{3}}, -\frac{1}{\sqrt{3}}, -\frac{1}{\sqrt{3}})$, $\vec{S}_3 = (-\frac{1}{\sqrt{3}}, \frac{1}{\sqrt{3}}, -\frac{1}{\sqrt{3}})$, $\vec{S}_4 = (-\frac{1}{\sqrt{3}}, -\frac{1}{\sqrt{3}}, \frac{1}{\sqrt{3}})$, where each direction corresponds to the four corners from the center of a tetrahedron. This non-coplanar spin structure gives the scalar chirality in eq.(1) locally. For the itinerant system γ -FeMn, a recent band structure calculation [20] concluded the stability of the triple-Q spin structure, in agreement with experiment [17].

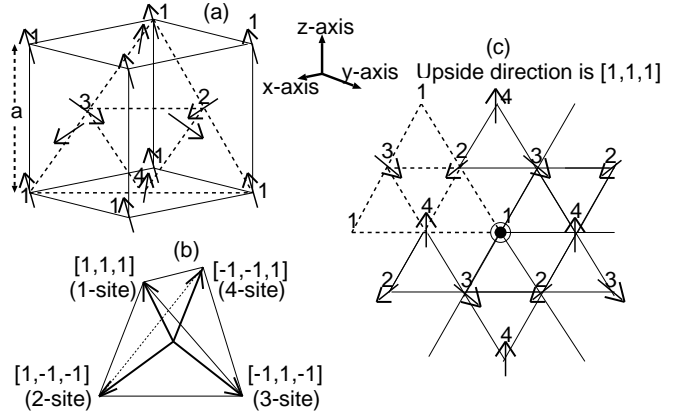


FIG. 1. (a) Triple-Q spin structure on fcc lattice. (b) Relation of the 4-spin moments \vec{S}_a ($a = 1, 2, 3, 4$). (c) Triangle lattice as a cross section of the fcc lattice perpendicular to [1,1,1]-direction.

Experimentally anomalous behaviors in the fcc AF are often observed. For example there occurs mysterious weak ferromagnetism (WF) in NiS₂ below the second AF transition temperature T_{N2} [21]. The Hall effect in this material is also large and strongly temperature dependent [22]. In Co(S_xSe_{1-x})₂, the AHE is enhanced in the intermediate x region, where the nontrivial magnetism is realized [23], and CeSb shows the largest Faraday rotation ever observed [24].

As shown below, the triple-Q AF state (Fig. 1a) on the distorted fcc lattice gives the orbital ferromagnetism accompanied by the AHE and even the realization of the three-dimensional quantum Hall liquid [25] *without* the external magnetic field.

The Hubbard on-site repulsive interaction U can be decomposed in terms of the Stratonovich-Hubbard transformation as

$$\frac{U}{2}\bar{\varphi}_i^2 - U\bar{\varphi}_i \cdot c_{i\alpha}^\dagger \bar{\sigma}_{\alpha\beta} c_{i\beta}, \quad (2)$$

where $\bar{\sigma}$ are the Pauli matrices and $\bar{\varphi}_i$ is the spin fluctuation field. This field acts as the local effective magnetic field for the electron, which can be regarded as the c-number in the mean field approximation for the magnetically ordered state. The symmetry properties of the ground state is captured by this approximation, and the quantized Hall effect discussed below is stable against the fluctuation of the $\bar{\varphi}$ -field as long as the gap does not collapse. Therefore we can consider this system as the free electron model in the background of the static field $U\bar{\varphi}_i$. In particular when this field $U|\bar{\varphi}_i|$ is much stronger than the transfer integrals t_{ij} 's, we can map the model into that of spinless fermions $H = -\sum_{ij} t_{ij}^{\text{eff}} f_i^\dagger f_j$ with the effective transfer integral

$$\begin{aligned} t_{ij}^{\text{eff}} &= t_{ij} \langle \chi_i | \chi_j \rangle \\ &= t_{ij} \left(\cos \frac{\theta_i}{2} \cos \frac{\theta_j}{2} + \sin \frac{\theta_i}{2} \sin \frac{\theta_j}{2} e^{-i(\phi_i - \phi_j)} \right), \end{aligned} \quad (3)$$

where $|\chi_i\rangle = [\cos \frac{\theta_i}{2}, \sin \frac{\theta_i}{2} e^{i\phi_i}]^t$ is the spin wavefunction and θ_i and ϕ_i are the polar coordinates of the spin direction. The phase factor appearing in t_{ij}^{eff} can be regarded as the gauge vector potential $a_\mu(\vec{r})$, and the corresponding gauge flux is related to χ_{ijk} in eq.(1) [5,6]. However, it should be noted here that the effective magnetic flux vanishes when averaged over the unit cell because of the periodicity of the vector potential $a_\mu(\vec{r}) = a_\mu(\vec{r} + \vec{T}_i)$ (\vec{T}_i : primitive vector). Therefore, the net effect of the gauge flux comes from the fact that there are more than two atoms and/or orbitals in the unit cell and the resultant multiband structure. Then each band is characterized by the Chern number [26]. The Chern number appears as a result of the spin-orbit interaction and/or the spin chirality in ferromagnets [11,27]. In ferromagnets the T-broken symmetry is manifest, while in AF the T-operation combined with the translation operation often constitutes the unbroken symmetry. In the latter case, the nonzero Hall conductivity σ_{xy} is forbidden. However when there are more than two sublattices and the spin structure is non-collinear, this combined symmetry would be absent and finite σ_{xy} is not forbidden.

In order to facilitate the understanding, first consider the triangular lattice, which is the (1,1,1)-cross section of the fcc lattice (Fig. 1c), and tight binding model with nearest neighbor hopping given in eq.(3) has the

gauge flux of $\pi/2$ penetrating each triangle. The unit cell is composed of eight triangles including four atoms. Thus the total gauge flux penetrating the unit cell is $4\pi \equiv 0 \pmod{2\pi}$, which is consistent with the periodicity of the lattice. The Chern number can be estimated analytically as $-\frac{e^2}{h}(\frac{e^2}{h})$ for the lower (higher) energy band. Therefore this two-dimensional spin configuration on the triangular lattice offers an example where the spin chirality orders without the ferromagnetic spin moment.

When one considers the three-dimensional fcc lattice, on the other hand, there are three other cross sections equivalent to [1,1,1]-direction, namely [-1,-1,1], [-1,1,-1], [1,-1,-1]. Therefore it is naturally expected that the net spin chirality is zero, because the spin chiralities are the vector quantities and the sum of these four vectors is zero. Actually $\sigma_{xy} = \sigma_{yz} = \sigma_{zx} = 0$ for the fcc lattice as shown below. However, this means that the chirality remains finite when the symmetry between the four directions is violated. For example, when the lattice is distorted along [1,1,1]-direction, it is expected that $\sigma_H = \sigma_{xy} = \sigma_{yz} = \sigma_{zx}$ becomes finite. We express the distortion along [1,1,1]-direction by putting the transfer integral within the (1,1,1)-plane as $t_{\text{intra}} = 1$, while that between the planes as $t_{\text{inter}} = 1 - d$ [28]. As the unit cell is cubic shown in Fig. 1a, the first Brillouin zone (BZ) is cubic: $[-\frac{\pi}{a}, \frac{\pi}{a}]^3$. From now on, we set $a = 1$. Then the Hamiltonian matrix $H(\vec{k})$ for each \vec{k} is given by

$$H(\vec{k}) = \begin{pmatrix} 0 & e^{-i\frac{\pi}{6}} f_2 & e^{i\frac{\pi}{6}} f_1 & f_3 \\ e^{i\frac{\pi}{6}} f_2 & 0 & e^{-i\frac{\pi}{6}} f_3 & e^{i\frac{2\pi}{3}} f_1 \\ e^{-i\frac{\pi}{6}} f_1 & e^{i\frac{\pi}{6}} f_3 & 0 & e^{-i\frac{2\pi}{3}} f_2 \\ f_3 & e^{-i\frac{2\pi}{3}} f_1 & e^{i\frac{2\pi}{3}} f_2 & 0 \end{pmatrix}, \quad (4)$$

where $f_1 = 2(1-d)\cos(\frac{k_z}{2} + \frac{k_x}{2}) + 2\cos(-\frac{k_z}{2} + \frac{k_x}{2})$, $f_2 = 2(1-d)\cos(\frac{k_x}{2} + \frac{k_y}{2}) + 2\cos(-\frac{k_x}{2} + \frac{k_y}{2})$, $f_3 = 2(1-d)\cos(\frac{k_y}{2} + \frac{k_z}{2}) + 2\cos(-\frac{k_y}{2} + \frac{k_z}{2})$. In this Hamiltonian, two bands ($\varepsilon_{1,2} = -\sqrt{f_1 + f_2 + f_3}$) and upper two bands ($\varepsilon_{3,4} = \sqrt{f_1 + f_2 + f_3}$) are completely degenerate. At $d = 0$, these two dispersions touch along the edge of the 1st BZ, i.e. $(k_x = \pm\pi, k_y = \pm\pi, k_z)$, $(k_x, k_y = \pm\pi, k_z = \pm\pi)$, $(k_x = \pm\pi, k_y, k_z = \pm\pi)$. Fixing k_z , for example, the \vec{k} -point $(k_x = \pm\pi, k_y = \pm\pi)$ is the center of the massless Dirac fermion (Weyl fermion) in (2+1)D. Therefore the band touching along the edge can be regarded as an assemble of the (2+1)D Weyl fermions. What happens for finite d differs for positive and negative values of d . For $d > 0$ (elongation along [1,1,1]-direction), all the Weyl fermions along the edges open a gap and turn into the massive Dirac fermions. Therefore the gap opens in the density of states centered at $\varepsilon = 0$. For $d < 0$ (suppression along [1,1,1]-direction), on the other hand, all the (2+1)D Weyl fermions along the edges open the gap; two (3+1)D Weyl fermions emerge instead at $(k_x, k_y, k_z) = \pm 2 \arcsin(\sqrt{\frac{4-2d}{4-4d}})(1, 1, 1) = \pm D(1, 1, 1)$

where \pm correspond to right- and left-handed chirality [8]. Here we consider the mass of the Dirac fermions at the edges of the BZ. For $d > 0$, the mass of the (2+1)D fermion along the k_μ -axis is positive for every k_μ , while that changes sign at $k_\mu = \pm D$ for $d < 0$.

Based on this observation, the transverse conductivity can be calculated in terms of the formula in [26]

$$\begin{aligned} \sigma_{xy} &= \sum_{n=1}^4 \int_{[-\pi:\pi]} \frac{dk_z}{2\pi} \int_{[-\pi:\pi]^2} \frac{dk_x dk_y}{2\pi i} f(\varepsilon_n(\vec{k})) (\nabla_{\vec{k}} \times \vec{A}_n(\vec{k}))_z \\ &= \frac{e^2}{h} \int_{[-\pi:\pi]} \frac{dk_z}{2\pi} \sigma_{xy}(k_z), \end{aligned} \quad (5)$$

where $f(\varepsilon)$ is the Fermi distribution function, and $\vec{A}_n(\vec{k}) = \langle n\vec{k} | \nabla_{\vec{k}} | n\vec{k} \rangle$ is the vector potential created by the Bloch wavefunction $|n\vec{k}\rangle$. Let us consider $\mu = 0$ case, i.e. quarter filled case. $\sigma_{xy}(k_z)$ is the Hall conductance in (2+1)D system with fixed k_z , which is determined by the parity anomaly caused by the Dirac fermions along the edge of the BZ. Explicit calculation shows at $T = 0\text{K}$, $\sigma_{xy}(k_z) = -\frac{e^2}{h} \text{sign}(f_2(k_z) \cdot d)$ where $f_2(k_z) \equiv (4 - 2d) \cos(\frac{k_z}{2})^2 + 2d \cdot \sin(\frac{k_z}{2})^2$. For $d > 0$, $\sigma_{xy}(k_z) = -\frac{e^2}{h}$ for all k_z , while $\sigma_{xy}(k_z) = \frac{e^2}{h}$ for $k_z = (-D, D)$ and $\sigma_{xy}(k_z) = -\frac{e^2}{h}$ for $k_z = [-\pi, -D)$ and $(D, \pi]$ in the case of negative $d < 0$. Integrating over k_z , we obtain $\sigma_{xy} = -\frac{e^2}{h}$ for $d > 0$ and $\sigma_{xy} = \frac{e^2}{h} \left[\frac{4}{\pi} \arcsin(\sqrt{\frac{4-2d}{4-4d}}) - 1 \right]$ for $d < 0$, while σ_{xy} vanish for $d = 0$. One can easily check that $\sigma_{xy} = \sigma_{yz} = \sigma_{zx} = \sigma_H$, and that the sign of σ_H changes when all the spins \vec{S}_a are inverted ($\vec{S}_a \rightarrow -\vec{S}_a$). One can confirm analytically in eq.(4) that the cancellation between the contributions from the two \vec{k} -points related by the parity (P) symmetry, e.g. (k_x, k_y, k_z) and $(-k_x, k_y, k_z)$, occurs and σ_{xy} is zero for the undistorted fcc lattice. This remains true even when we modify \vec{S}_a from those given in Fig. 1b. For example even with finite magnetization ($\sum_{a=1}^4 \vec{S}_a \neq \vec{0}$), $\sigma_{xy}(\omega) = 0$ for any ω on the undistorted fcc lattice. In short, P-symmetry is not broken while T-symmetry is broken in the undistorted fcc lattice, where finite σ_H is forbidden. An distortion along [1,1,1]-direction *does* break this P-symmetry and produces finite σ_H .

Next we turn to the half filled case. When the chemical potential is in the Mott gap, i.e. Mott insulator, the d.c. σ_H vanishes. However the optical $\sigma_H(\omega)$ can be finite, which corresponds to the Faraday and/or the Kerr rotation. In order to calculate $\sigma_H(\omega)$, we have to take into account optical transitions between the lower and the upper Hubbard bands. In the mean field picture, this corresponds to the two splitted bands due to the effective magnetic field $U|\vec{\varphi}_i$ in eq.(2). Diagonalizing the tight-binding Hamiltonian with this local ‘‘magnetic field’’, we can calculate $\sigma_H(\omega)$. $\sigma_H(\omega)$ shown in Fig. 2 is for $d = -0.1, U|\vec{\varphi}_i| = 5$.

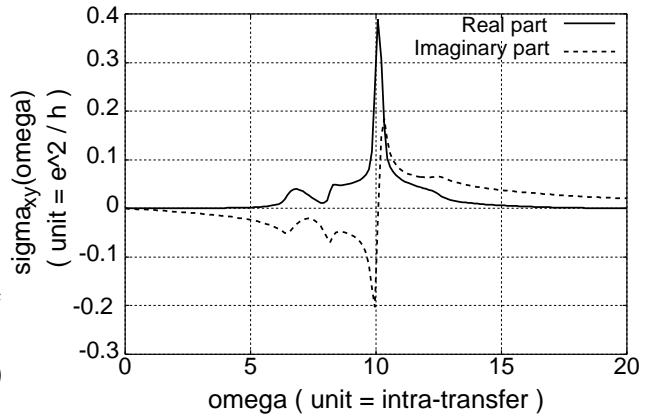


FIG. 2. $\sigma_H(\omega)$ for $d = -0.1, U|\vec{\varphi}_i| = 5$

Now we turn to the orbital ferromagnetism induced by the distortion. Orbital magnetization M is given by

$$M = \lim_{B \rightarrow 0} \int_{-\infty}^{\epsilon_F} \frac{\partial N(B, \mu)}{\partial B} d\mu. \quad (6)$$

In terms of the Středa formula [29], i.e. $\sigma_{xy}|_\mu = \sigma_{xy}^I|_\mu + ec \frac{\partial N(B, \mu)}{\partial B}$ with $\sigma_{xy}^I|_\mu = i \frac{1}{2\hbar} \text{Tr}[\hat{J}_x G^+(\mu) \hat{J}_y \delta(\mu - H) - \hat{J}_x \delta(\mu - H) \hat{J}_y G^-(\mu)]$, we estimate the integrand in eq.(6) from $\sigma_{xy}|_\mu$ and $\sigma_{xy}^I|_\mu$.

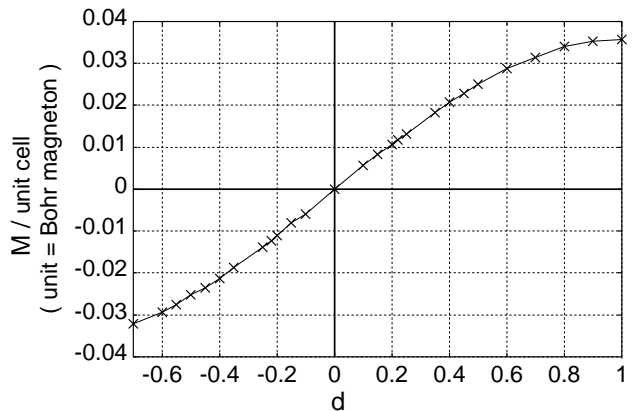


FIG. 3. Magnetization M as a function of d , where $U|\vec{\varphi}_i| = 5$ (we set $\frac{\hbar^2}{ma^2} \sim t_{\text{intra}} = 1$)

Shown in Fig. 3 is the orbital magnetization M as a function of the distortion d for the half filled case. The sign of orbital magnetization M changes when all the spins are inverted. (Magnetization depicted in Fig. 3 corresponds to the triple-Q structure in Fig. 1a,b.) Note that M is finite even though the d.c. $\sigma_H = 0$ in this case, because the former is determined by the integral over the occupied states.

In real materials, the configuration with all the spins being inverted (which means that the chirality is also inverted) has the same energy. Thus it is expected that the

domain structure of these two chiralities is formed. In order to align this chiral domain, we must cool down into AF order phase by applying external strain *and* external magnetic field, which couples to the orbital magnetization and prefers one of the chiral domain. (For $d > 0$, the magnetic field in [1,1,1]-direction prefers the triple-Q structure as in Fig. 1a,b.) Lastly it is noted here that the distortion along [1,1,0] or other three equivalent directions produces the similar effect as discussed above, while that along [1,0,0] etc. does not. This also offers a way to test this idea experimentally.

Now we discuss the experimental relevance of these results. One of the most promising materials for this spin chirality mechanism is the itinerant AF γ -Fe_xMn_{1-x} alloy as mentioned above [17]. In this material, the triple-Q structure is observed for $0.35 < x < 0.8$. This material remains metallic even below T_N . Because the crystal structure is the undistorted fcc, one needs to apply uniaxial stress toward the [1,1,1] or [1,1,0]-direction. Although the band structure is rather complicated and there is no gap in the density of states [20], we expect the transverse conductivity σ_H of the order of $e^2 d/ha \cong 1400d\Omega^{-1}\text{cm}^{-1}$ for $a = 3.6\text{\AA}$ when the chiral domains are aligned by the field cooling.

Another candidate is the CT insulator AF NiS₂. In this material the valence of Ni is 2+, and the angular orbital moment is quenched with d^8 configuration. Thus spin-orbit interaction is expected to be small, and this material is an ideal laboratory to study the spin chirality mechanism. It shows two successive magnetic phase transitions at $T_{N1} = 40\text{K}$ and $T_{N2} = 30\text{K}$. Between T_{N1} and T_{N2} , the magnetic structure is given by Fig. 1a,b (type I AF state). At T_{N2} the type II AF structure appears in addition to the type I structure. This is accompanied by the rhombohedral distortion and with the mysterious WF [21]. This lattice distortion ($d > 0$) lifts the quasi-degeneracy of type I and type II structures [30]. This brings about finite orbital ferromagnetism, which can be detected by hysteresis in the magnetization curve under the magnetic field. Therefore the present results give a possible scenario for the WF in NiS₂. Even in the temperature range between T_{N1} and T_{N2} , where lattice is not distorted spontaneously, suppression toward [1,1,1] or [1,1,0]-direction is predicted to bring about an orbital ferromagnetism. (The compressibility of this material is of the order of 10^{-3}kbar^{-1} [31] and we need $\sim 140\text{kbar}$ uniaxial pressure to produce $d = -0.1$ for example.) Although the d.c. $\sigma_H(\omega)$ is zero at $T = 0\text{K}$, the optical $\sigma_H(\omega)$ is expected to be finite, as shown in Fig. 2. As for other fcc AF such as Co(S_xSe_{1-x})₂, detailed studies on the spin structure by neutron scattering are highly desirable, with which the mechanism of the Hall effect can be dictated.

The authors acknowledges Y. Tokura, Y. Endoh, A. Mishchenko, M. Onoda and Y.Taguchi for fruitful discussions. N.N. is supported by Priority Areas Grants

and Grant-in-Aid for COE research from the Ministry of Education, Culture, Sports, Science and Technology of Japan.

-
- [1] J. Villain, J. Phys. C **10**, 1717 and 4793 (1977).
 - [2] S.Miyashita and H.Shiba, J. Phys. Soc. Jpn. **53**, 1145 (1984); Prog. Theor. Phys. Suppl. **87** 112 (1986).
 - [3] H. Kawamura, Phys. Rev. Lett. **80**, 5421 (1998).
 - [4] V. Kalmeyer and R. B. Laughlin, Phys. Rev. Lett. **59**, 2095 (1987); R. B. Laughlin, *ibid* **60**, 2677 (1998).
 - [5] X. G. Wen, F. Wilczek and A. Zee, Phys. Rev. **B39**, 11413 (1989).
 - [6] P. A. Lee and N. Nagaosa, Phys. Rev. **B46**, 5621 (1992).
 - [7] S. Deser, R. Jakiew, and S. Templeton, Phys. Rev. Lett. **48**, 975 (1982); R. Jakiew, Phys. Rev. D **29**, 2375 (1984).
 - [8] H. B. Nielson and M. Ninomiya, Phys. Lett. **130B**, 389 (1983);
 - [9] R. B. Laughlin, Phys. Rev. Lett.**60**, 2677 (1988).
 - [10] F. D. M. Haldane Phys. Rev. Lett. **61**, 2015(1988).
 - [11] K. Ohgushi, S. Murakami, and N. Nagaosa, Phys. Rev. **B62**, R6065 (2000).
 - [12] P. Matl et al., Phys. Rev. **B57**, 10248 (1998).
 - [13] S. H. Chun et al., Phys. Rev. Lett. **84**, 757 (2000).
 - [14] Jinwu Ye *et al.*, Phys. Rev. Lett. **83**, 3737 (1999).
 - [15] Y. Taguchi et al., Science **291**, 2573 (2001).
 - [16] J. A. Wilson ,and G. D. Pitt, Phil. Mag. **23**,1297 (1971); K. Kikuchi et al., J. Phys. Soc. Jpn. **45**, 444 (1978).
 - [17] Y. Endoh and Y. Ishikawa, J. Phys. Soc. Jpn. **30**, 1614 (1971).
 - [18] K. Yoshida , and S. Inagaki J. Phys. Soc. Jpn. **50**, 3268 (1980).
 - [19] A. Yoshimori, and S. Inagaki J. Phys. Soc. Jpn. **50**, 769 (1981).
 - [20] A. Sakuma , J. Phys. Soc. Jpn. **69**, 3072 (2000).
 - [21] T. Thio, J. W.Benett, and T. R. Thurston, Phys. Rev. **B52**, 3555 (1995).
 - [22] T. Thio and J. W. Bennett, Phys. Rev. **B50**, 10574 (1994).
 - [23] K. Adachi, M. Matsui, and Y. Omata, J. Phys. Soc. Jpn. **50**, 83 (1981).
 - [24] R. Pittini et al., Phys. Rev. Lett. **77**, 944 (1996).
 - [25] M. Kohmoto, B. Halperin and Y-S. Wu, Phys. Rev. **B45**, 13488 (1992);B. I. Halperin, J. Journal of Applied Phys. **26** (Suppl.), 1913 (1987)).
 - [26] D. J. Thouless et al., Phys. Rev. Lett. **49**, 405 (1982); M. Kohmoto, Ann. Phys. (N.Y.) **160**, 343 (1985).
 - [27] M. Onoda, and N. Nagaosa, to be published.
 - [28] The change of J_4 due to the distortion will change \vec{S}_i ($i = 1 - 4$), and hence the effective transfer integral t_{ij}^{eff} . However this does not give the finite σ_{xy} as long as the bare transfer integral t_{ij} remains unchanged.
 - [29] P. Středa , J. Phys. C. Solid State Phys. **15**, L717 (1982).
 - [30] M. Matsuura et al., unpublished.
 - [31] S. Endo, T. Mitsui, and T. Miyadai , Phys. Lett. **46A**, 29 (1973).